was rapid not just around Greenland but was also nearly synchronous over a large part of the terrestrial biosphere (*24*, *25*).

A hemisphere-wide increase in water vapor at the onset of the transition is suggested by the increase in methane source areas, a possible increase in particle washout rate and decreased size of dust source areas, and increased snow accumulation at Summit. Although it is unclear if the change in environmental conditions resulting in the increase in methane led temperature change in Greenland, other climate proxies associated with non-Arctic areas (deuterium excess, non–sea-salt calcium, and particle concentration) appear to change before climate proxies associated with Arctic areas and Arctic atmospheric transport (δD, sea-salt sodium, and mean particle size). This difference suggests that some climate conditions changed outside of the Arctic in 11,660 B.P. and were followed by changes at higher latitudes in 11,645 and 11,612 B.P. Because the proxy records that are available are not sensitive to all of the climate changes occurring in the Arctic, it is not clear if the climate transition started at lower latitudes or if earlier changes that we are unable to detect occurred in more northern regions.

We speculate that the transition was characterized by a change in ocean circulation that significantly increased atmospheric water vapor. This added vapor could have increased retention of long-wave solar radiation and created a feedback that stabilized the new climate state. Regardless of the mechanism, the transition was a 50-year period during which wind speeds, precipitation, temperatures, and sea ice were changing throughout the Northern Hemisphere on subdecadal time scales.

REFERENCES AND NOTES

1. P. M. Grootes, M. Stuiver, J. W. C. White, S. Johnsen, J. Jouzel, *Nature* **366**, 552 (1993).
2. S. J. Johnsen *et al.*, *ibid.* **359**, 311 (1992).
3. K. C. Taylor, *et al.*, *ibid.* **366,** 549 (1993).
4. R. B. Alley *et al.*, *ibid.* **362**, 527 (1993).
5. D. A. Meese *et al.*, *Science* **266**, 1680 (1994); D. A. Meese *et al.*, *J. Geophys. Res.*, in press.
6. P. A. Mayewski, W. B. Lyons, M. J. Spencer, *Nature* **346**, 554 (1990).
7. P. Y. Whung, E. S. Saltzman, M. J. Spencer, P. A. Mayewski, N. Gundestrup, *J. Geophys. Res.* **99**, 1157 (1994).
8. K. C. Taylor *et al.*, *Nature* **361**, 432 (1993).
9. K. C. Taylor *et al.*, *J. Glaciol.* **38**, 325 (1992).
10. E. W. Wolff *et al.*, *J. Geophys. Res.* **100**, 16249 (1995).
11. A. Neftel, M. Andrée, J. Schwander, B. Stauffer, C. U. Hammer, *Geophys. Monogr. Am. Geophys. Union* **33**, 32 (1985).
12. G. A. Zielinski, P. A. Mayewski, L. D. Meeker, S. Whitlow, M. S. Twickler, *Quat. Res.* **45**, 109 (1996).
13. J. W. C. White *et al.*, *J. Geophys. Res.*, in press.
14. P. A. Mayewski *et al.*, *Science* **261**, 195 (1993).
15. J. W. C. White, S. J. Johnsen, W. Dansgaard, *Ann. Glaciol.* **10**, 219 (1977); S. J. Johnsen, W. Dansgaard, J. W. C. White, *Tellus B* **41**, 453 (1989).
16. J. R. Petit, J. W. C. White, N. W. Young, J. Jouzel, Y. S. Korotkevich, *J. Geophys. Res.* **96**, 5113 (1991).
17. W. Dansgaard, J. W. C. White, S. J. Johnsen, *Nature* **339**, 532 (1989).
18. G. A. Zielinski and G. R. Mershon, *Geol. Soc. Am. Bull.* **109**, 547 (1997).
19. W. R. Kapsner, R. B. Alley, C. A. Shuman, S. Anandakrishnan, P. M. Grootes, *Nature* **373**, 52 (1995).
20. P. A. Mayewski *et al.*, *Science* **263**, 1747 (1994).
21. P. A. Mayewski, M. J. Spencer, W. B. Lyons, M. S. Twickler, *Atmos. Environ.* **21**, 863 (1987); P. A. Mayewski *et al.*, *Science* **272**, 1636 (1996); S. R. O'Brien *et al.*, *ibid.* **270**, 1962 (1995); S. Whitlow, P. A. Mayewski, J. E. Dibb, *Atmos. Environ. A* **26**, 2045 (1992); Q. Yang, P. A. Mayewski, E. Linder, S. Whitlow, M. Twickler, *J. Geophys. Res.* **101**, 18629 (1996).
22. P. J. Fawcett, A. M. Agustdottir, R. B. Alley, C. A. Shuman, *Paleoceanography* **12**, 23 (1997).
23. K. M. Cuffey, R. B. Alley, P. M. Grootes, J. M. Bolzan, S. Anandakrishnan, *J. Glaciol.* **40**, 341 (1994).
24. J. P. Severinghaus, T. Sowers, E. J. Brook, R. B. Alley, M. L. Bender, *Nature*, in press.
25. E. J. Brook, T. Sowers, J. Orchardo, *Science* **273**, 1087 (1996).

26. This work was funded by the Office of Polar Programs, National Science Foundation. We thank the GISP2 Science Management Office at the University of New Hampshire, the Polar Ice Coring Office (located at the University of Alaska when the drilling was done, and currently at the University of Nebraska), and the TAG 109 New York Air National Guard.

24 June 1997; accepted 27 August 1997

The Impact of Aerosols on Solar Ultraviolet Radiation and Photochemical Smog

R. R. Dickerson,* S. Kondragunta, G. Stenchikov, K. L. Civerolo, B. G. Doddridge, B. N. Holben

Photochemical smog, or ground-level ozone, has been the most recalcitrant of air pollution problems, but reductions in emissions of sulfur and hydrocarbons may yield unanticipated benefits in air quality. While sulfate and some organic aerosol particles scatter solar radiation back into space and can cool Earth's surface, they also change the actinic flux of ultraviolet (UV) radiation. Observations and numerical models show that UV-scattering particles in the boundary layer accelerate photochemical reactions and smog production, but UV-absorbing aerosols such as mineral dust and soot inhibit smog production. Results could have major implications for the control of air pollution.

More than 100 counties in the United States regularly violate the Environmental Protection Agency's (EPA) Ambient Air Quality Standard for ozone (O_3) of 120 ppbv (parts per 10^9 by volume averaged over 1 hour) (*1*). This ozone results from the interaction of pollutant oxides of nitrogen and nonmethane hydrocarbons (NMHCs) with solar radiation, for example, via reactions (1) to (4), and is thus sometimes called photochemical or Los Angeles–type smog.

$$\mathrm{NMHC} + \mathrm{OH} + \mathrm{O_2} \rightarrow \mathrm{RO_2} + \mathrm{H_2O} \quad (1)$$

$$\mathrm{RO_2} + \mathrm{NO} + \mathrm{O_2} \rightarrow \mathrm{NO_2} + \mathrm{HO_2} + \mathrm{CARB} \quad (2)$$

$$\mathrm{HO_2} + \mathrm{NO} \rightarrow \mathrm{NO_2} + \mathrm{OH} \quad (3)$$

$$2(\mathrm{NO_2} + h\nu + \mathrm{O_2} \rightarrow \mathrm{NO} + \mathrm{O_3}) \quad (4)$$

$$\text{net: } \mathrm{NMHC} + 4\mathrm{O_2} + 2h\nu \rightarrow 2\mathrm{O_3} + \mathrm{CARB}$$

(where CARB is carbonyl compounds, which can further break down to produce additional O_3, and $h\nu$ represents a quantum of light). The rate of production of smog depends on the concentrations of these pollutants and [for reactions such as (4)] on the intensity of solar near-UV ($300 < \lambda < 400$ nm) radiation (*2*, *3*).

On hot, smoggy summer days in many North American and European cities the cloud-free sky shows a milky white color—the result of particulate air pollution scattering solar radiation. The impact of these aerosols on Earth's radiative balance and on climate (aerosol radiative forcing) has been studied extensively (*4*). The amount of radiation available to drive these reactions depends on the solar zenith angle (θ), absorption and scattering by gases and particles, and the surface albedo (the fraction of light reflected from Earth's surface). In the atmosphere, ozone is usually the only important absorbing gas in the near-UV spectrum. Scattering of radiation by gases (Rayleigh scattering) redistributes much of the UV radiation; Bruehl and Crutzen (*5*) showed that Rayleigh scattering can increase the effective path length and relative importance of tropospheric ozone in shielding us from harmful UV radiation. Optically thick clouds reduce the radiation below them, but calculations by Madronich (*6*) showed that scattering by cloud droplets can actually increase the actinic flux and the rate of photochemical reactions in the upper parts of clouds.

Theoretical calculations and observa-

R. R. Dickerson, S. Kondragunta, G. Stenchikov, K. L. Civerolo, B. G. Doddridge, Department of Meteorology, University of Maryland, College Park, MD 20742, USA. B. N. Holben, NASA Goddard Space Flight Center, Greenbelt, MD 20742, USA.

*To whom correspondence should be addressed. E-mail: russ@atmos.umd.edu

tions of photolysis rates under clear skies agree well (*2*, *3*, *6*), but observations in clouds or aerosol layers are few (*7*). There have been estimates of the effects of aerosols on UV flux, but only now are simultaneous observations of aerosol loading, size number distributions, and photochemistry available to determine the impact of aerosols on UV flux and smog formation. We now present results from observations and computer simulations showing that scattering by aerosols can have a substantial, and counterintuitive, impact on the flux of UV radiation and the production of ground-level ozone.

The aerosol optical depth (τ) and the photolysis rate coefficient $j(NO_2)$ were measured from July to September 1995 on the grounds of the NASA Goddard Space Flight Center (GSFC), in Greenbelt, Maryland (39°N). This suburban site, located between Washington, D.C., and Baltimore, Maryland, is the frequent recipient of high levels of photochemical smog. For studies of ozone formation, we will focus on a severe smog episode that struck the eastern United States on 13 to 15 July 1995. This episode was studied extensively as part of the field campaign of the North American Research Strategy for Tropospheric Ozone–Northeast (NARSTO-NE) (*8*).

Optical depth and column aerosol properties were inferred from nearly continuous observations of solar radiation at four to six wavelengths (*9*). Aerosol loading and light extinction at GSFC are typical of the mid-Atlantic region (*1*, *10*). Radiation observations were mathematically inverted to obtain the aerosol size-number distribution used as input for our calculations of aerosol optical characteristics. The photolysis rate coefficient $j(NO_2)$ was measured directly with a chemical actinometer (*7*).

Numerical models were used to calculate aerosol optical properties, photolysis rate coefficients, and ozone concentration. For the retrieval algorithm we assumed that aerosol particles have a refractive index (m) of $1.45 - 0.005i$. The refractive index of aerosol particles is described by a complex number, where the real part of m is related to scattering, the imaginary part to absorption. This refractive index agrees with estimates for the East Coast aerosol composed predominantly of sulfates, organic compounds, and nitrates [themselves products of photochemical reactions (*11*)] with minor contributions from graphitic carbon ("soot") and mineral dust (*10*, *12*). Sulfuric acid absorbs much less radiation ($m = 1.44 - 1.0 \times 10^{-8}i$) than does mineral dust ($m = 1.53$ to $0.008i$) or soot ($m = 1.75$ to $0.465i$).

We used retrieved aerosol size-number distribution and a numerical package based on Mie theory (*13*) to calculate the extinction coefficient, single-scattering albedo (ω), phase function, and asymmetry factor. The results were used to recalculate τ at 380 nm; the favorable comparison with direct measurements demonstrates internal consistency (*9*).

The derived aerosol properties were then used as input to the discrete ordinate radiative transfer (DISORT) model (*14*) for calculation of actinic flux and, in combination with molecular properties, photolysis rate coefficients (*15*, *16*). For comparison to direct measurements, $j(NO_2)$ was calculated with local albedo set to match the actinometer albedo of zero. For calculation of smog production, the model albedo was set to match the albedo of Earth's surface, 4 to 8%. We conducted multiple calculations to investigate the sensitivity of $j(NO_2)$ to solar zenith angle, aerosol optical depth, refractive index, and the distribution of the aerosol with altitude.

The latest in a series of EPA-sponsored photochemical smog models is the variable-grid urban airshed model (UAM-V), a three-dimensional Eulerian grid model, developed for EPA to test the efficacy of plans for reducing photochemical smog (*1*). In the model, there are 137 by 110 fine grid cells nested into 64 by 63 coarse grid cells in the x-y plane. The dimensions of the fine and coarse grid cells are 12 km by 12 km and 36 km by 36 km, respectively. The UAM-V uses meteorological observations from the National Weather Service and internally consistent equations of fluid dynamics to calculate advection and dispersion. A photochemical subroutine that makes use of emissions inventories and with 39 species in 91 gas-phase reactions calculates concentrations of ozone and other trace gases for each of the seven vertical layers. Calculated concentrations agreed reasonably well with observations of ozone and oxides of nitrogen (*8*). Although the actual process of smog formation is complicated and highly nonlinear, this model can provide a reasonable test of the impact of changing a single variable, in this case UV flux.

Results from radiometric measurements made at NASA GSFC show very high τ at the photochemically active wavelengths of 339, 380, and 440 nm (all τ values hereafter refer to 380 nm). For example, on 35 days in 1995 when maximum hourly average ozone mixing ratio exceeded 100 ppbv, τ averaged near unity. Over the course of the 1995 smog season (April to September), τ and maximum ozone correlated positively ($r = 0.66$) with a slope of 31 ppbv per unit optical depth.

A direct comparison of theory and experiment can be made for periods of simultaneous observations of column aerosol properties and surface $j(NO_2)$. Data collected in the summer of 1995 (Fig. 1) show excellent agreement over a broad range of optical depths and zenith angles. Lowest values of $j(NO_2)$ correspond to greatest values of τ and θ. The close fit of calculated and measured photolysis rate coefficients shows that Mie theory and the DISORT model correctly treat scattering and absorption and their zenith angle dependence. This agreement gives us confidence in the model's ability to predict the impact of aerosols on $j(NO_2)$ under other conditions and at other altitudes.

We can use the model to learn what controls the impact of aerosols on UV flux and photolysis rates (Fig. 2). The highest photolysis rate coefficients are obtained for a cloud and aerosol-free atmosphere (line a). Purely scattering aerosols (line b) have no discernible effect on $j(NO_2)$ when the sun is near the zenith (low θ), but reduce the actinic flux at higher θ. Observed aerosols have very low absorption. Previous estimates of m for aerosols observed over the eastern United States center around 1.45 to $0.005i$ ($\omega = 0.96$) (*12*). Radiation striking such a particle has a 96% probability of being scattered and a

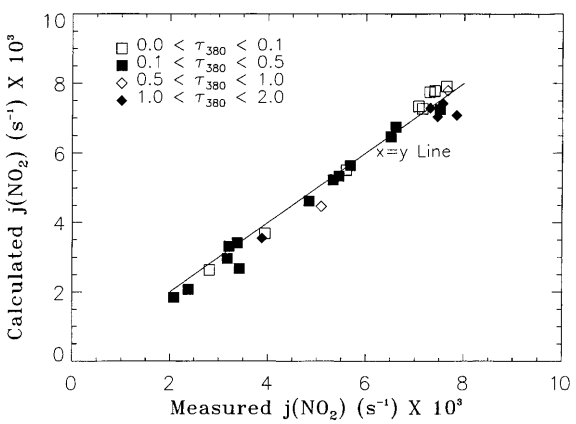

Fig. 1. Measured and calculated $j(NO_2)$ for a broad range of θ and τ for July and September 1995 at GSFC. Aerosol optical depths were measured nearly continuously, but the full suite of observations necessary for retrieval of aerosol properties were made only once or twice a day. The data plotted reflect simultaneous observations of $j(NO_2)$ and aerosol properties and show agreement within experimental uncertainty. This agreement also offers independent confirmation of the retrieval algorithm.

4% probability of being absorbed. For aerosol properties closest to observations (lines c and d), $j(NO_2)$ shows greater attenuation with increasing θ and τ. For constant τ, a higher imaginary index of refraction (greater absorption) reduces photolysis rate coefficients by a nearly constant amount at all θ studied (line e).

The θ dependence of the impact of aerosols on UV flux apparently results from the relative contributions of direct and diffuse (scattered) radiation. DISORT calculations indicate that under an aerosol-free atmosphere, diffuse radiation accounts for about 45% of the total actinic flux at 380 nm. For a τ of 1.26 (typical for smoggy conditions), this value rises to about 90%. Scattering reduces the direct beam, but at low θ diffuse radiation compensates for this loss. Higher effective optical depths ($\tau/\cos\theta$) attenuate both the direct and diffuse beams (*2*, *3*, *16*).

During the July 1995 smog episode, ozone levels reached 175 ppbv in the New York area on the 14th and 179 ppbv in Baltimore on the 15th. The meteorological conditions leading to the episode were well characterized and reasonably typical for multiday high-ozone events in the East Coast states (*8*). The skies were mostly cloud-free, but τ ranged from 1 to 2. The directly measured values of $j(NO_2)$ generally fall between lines c and d of Fig. 2. The observed $j(NO_2)$ shows the same strong dependence on θ predicted by the model for aerosols with a high ω. The scatter in the observed $j(NO_2)$ reflects the variability in τ throughout the day.

Altitude profiles of $j(NO_2)$ for an aerosol-free atmosphere and various values of τ (Fig. 3) show that our model calculations agree with direct measurements in the lower and middle troposphere. For typical eastern United States aerosol loadings, more UV radiation is available overall to drive photochemical reactions. Light that would have been absorbed by Earth's surface is scattered back into the atmosphere, increasing the effective path length of radiation. Most pollutants are emitted into the lowest kilometer or so of the atmosphere, called the planetary boundary layer (BL). During air pollution episodes, a strong temperature inversion usually isolates the BL from the rest of the troposphere, but within the BL vertical mixing is relatively rapid, that is, on the order of hours or less. The results presented in Fig. 3 show how the aerosols can greatly accelerate the rate of photolysis of NO_2 in the BL taken as a whole, and in the free troposphere.

To test the impact of these faster photolysis rates on ozone formation, we used the UAM-V with the observations of the 13 to 15 July 1995 episode as input (*8*). The model was run with altitude-dependent photolysis rate coefficients [for example, $j(NO_2)$, $j(O_3)$, $j(H_2O_2)$, and $j(H_2CO)$] calculated with DISORT for an aerosol-free atmosphere (a control run), and then for the observed aerosol loading ($\tau = 2$; $m = 1.45 - 0.005i$). Aerosol particles were assumed to be confined to the BL and distributed uniformly over the domain. The trace gas concentrations calculated with UAM-V agreed reasonably well with field and aircraft measurements (*8*).

Our UAM-V simulation (Fig. 4) shows that aerosol scattering of UV radiation can increase BL ozone mixing ratios by 20 ppbv or more. This represents an increase of about one-third in the amount of ozone produced over the 3-day model run. The greatest differences were observed over and downwind of New York City where maximum ozone was detected on 14 July 1995. As a sensitivity study, we ran the model for a purely scattering aerosol ($m = 1.45$ to $0.0i$; $\omega = 1.00$) to determine the maximum possible effect. Increases in ozone of up to 45 ppbv were generated.

To determine the impact of aerosols

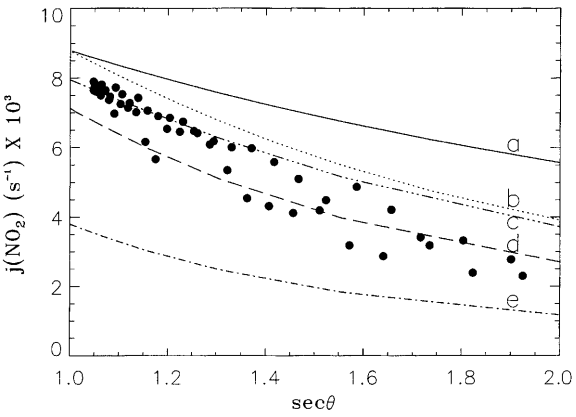

Fig. 2. Ground-level photolysis rate coefficients, $j(NO_2)$, as a function of the inverse of the cosine of the solar zenith angle (sec θ). For an overhead sun, the zenith angle is zero, and sec(θ) is unity; sec(60°) = 2.00. For these calculations and observations, the sun was unobstructed by clouds. The lines show calculated $j(NO_2)$ for the following conditions: a: $\tau = 0.00$, clear sky, no aerosol; b: $\tau = 1.00$, $m = 1.45 - 0.0i$, $\omega = 1.00$; c: $\tau = 1.00$, $m = 1.45 - 0.005i$, $\omega = 0.96$; d: $\tau = 2.00$, $m = 1.45 - 0.005i$, $\omega = 0.96$; e: $\tau = 2.00$, $m = 1.45 - 0.05i$, $\omega = 0.75$. Points are observations from 15 July 1995 during an East Coast smog event when τ ranged from 1 to 2.

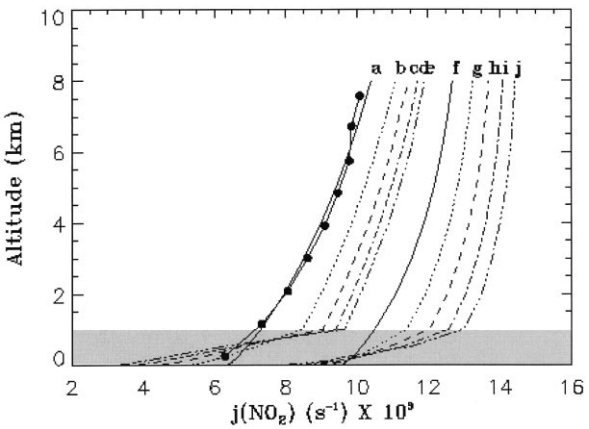

Fig. 3. Altitude profiles of $j(NO_2)$ calculated for $\theta = 58°$ (a to e) and 0° (f to j). Lines a and f represent the photolysis rate coefficients calculated for an aerosol-free atmosphere; dots represent clear-sky observations (*7*). Lines b to e and g to j indicate $j(NO_2)$ for τ of 0.5 to 2.0 in increments of 0.5. The aerosol ($m = 1.45 - 0.005i$) was assumed to be uniformly distributed through the first 1000 m of the atmosphere (gray area). Aerosols reduce the available UV radiation near the surface, but increase it substantially a few hundred meters above.

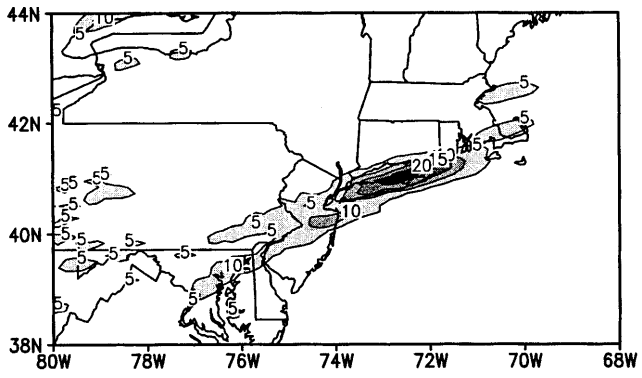

Fig. 4. Increases in ozone mixing ratios (averaged in 0 to 500 m altitude after 60 hours into the UAM-V model simulation that began at 0000 hours on 12 July 1995) as a result of scattering ($\Delta\tau = 2.0$) of solar UV radiation; contours are in increments of 5 ppbv. Results suggest that reduced sulfate loading can produce beneficial effects in reducing photochemical smog.

that more strongly absorb UV radiation, we ran the UAM-V for the same scenario, but with photolysis rate coefficients appropriate for a more strongly absorbing aerosol in the BL ($m = 1.45 - 0.05i$; $\omega = 0.75$). Changes in ozone mixing ratios were nearly the same in amount and location as those of Fig. 4, but opposite in sign. UV-absorbing aerosol reduced calculated ozone mixing ratios by up to 24 ppbv. Such reductions were also computed for an optically thick aerosol layer located above the boundary layer; this effect was seen for scattering as well as absorbing particles.

In this study, we have isolated the radiative impact of particulate pollution, but heterogeneous reactions are almost certainly important in tropospheric chemistry. Their impact remains highly uncertain. NO_x and HO_x reactions in cloud droplets and on sulfate particles can inhibit ozone production (*17*). Soot, by contrast, has been suggested to reduce HNO_3 to NO_x, increasing the potential to produce ozone (*18*). If aqueous-phase reactions of SO_2 and H_2O_2 reduce odd hydrogen in the atmosphere, this process could act as negative feedback on ozone formation. Conversely, increased radiation can increase the production of OH and H_2O_2 and thus oxidation of SO_2 to sulfate. For the conditions of Fig. 4, calculated H_2O_2 concentrations throughout the domain were about 0.8 ppbv (about 10%) higher with aerosols than without. Greater UV flux in the BL accelerates the rate of production of secondary sulfate and organic aerosol. These represent positive-feedback mechanisms between particles and ozone.

Scattering aerosols tend to cool the BL and stabilize the atmosphere with respect to convection. Lower temperatures lead to less smog, but greater stability leads to more smog. Absorbing aerosols in the BL destabilize the atmosphere, but aerosols in the free troposphere stabilize the atmosphere (*4*, *8*). Aerosol particles can also affect cloud microphysics and thus indirectly impact on atmospheric stability and radiation (*4*).

The radiative impact of aerosols on photochemical ozone formation could be important in other parts of the world. In Europe, the UV flux is generally lower than in the United States, but sulfate loading is high, and reducing sulfur emissions should reduce smog formation. In India, however, the UV flux is generally high, especially in the dry season of January to May. Available data show generally high concentrations of ozone precursors NO_x, NMHC, mineral dust, and soot (with extensive layers of absorbing aerosol in the dry season) but relatively low concentrations of ozone (*19*). These absorbing aerosols may reduce the UV flux enough to inhibit photochemical smog formation.

Over the past decade a modest (~ 6%) downward trend in ozone has been detected for the United States. Emissions of reactive nitrogen have not changed significantly, and the reduction in ozone has been attributed to concomitant reductions (9%) in NMHC emissions (*1*). Emissions of sulfur over the same time period have decreased by 18%, and future work on trends should address both changes. It is possible that continued reductions in the amount of sulfur in the atmosphere will have an unanticipated benefit of reducing low-level ozone concentrations.

REFERENCES AND NOTES

1. Photochemical production of tropospheric ozone has been studied extensively [J. H. Seinfeld, *Science* **243**, 745 (1989); National Academy of Sciences, *Rethinking the Ozone Problem in Urban and Regional Air Pollution* (National Academy of Sciences, Washington, DC, 1991); U.S. Environmental Protection Agency, *National Air Quality and Emissions Trends Report, 1995* (EPA454/R-96-005, 1996); B. J. Finlayson-Pitts and J. N. Pitts Jr., *Science* **276**, 1045 (1997). The effect of aerosols on UV flux and photochemical ozone production near Earth's surface has generally been assumed to be small and negative, that is, the presence of aerosols reduces slightly the rate of smog formation [L. Zafonte, P. Rieger, J. Holmes, *Environ. Sci. Technol*. **11**, 483 (1977); S. Liu, S. McKeen, S. Madronich, *Geophys. Res. Lett*. **18**, 2265 (1991); Y. Lu and M. A. K. Khalil, *Chemosphere* **32**, 739 (1996)]. Operation of many smog models, such as the Urban Airshed Models, is generally conducted without regard to the radiative effects of aerosols [U.S. Environmental Protection Agency, *Guidelines for Regulatory Application of Urban Airshed Model* (EPA-450/4-91-013, 1991); SAI, *Users Guide to the Variable Grid Urban Airshed Model (UAM-V)* (Systems Applications International, San Rafael, CA, 1995); R. Pielke *et al*., *Meteorol. Atmos. Phys*. **49**, 69 (1992)].
2. Photochemical reactions progress at a rate that depends on the intensity of radiation. For any particular species, the photolysis rate coefficient can be calculated by integrating the product of the actinic flux, the quantum yield, and the absorption cross section with respect to wavelength. This coefficient can also be measured directly with a chemical actinometer. See, for example, J. Peterson and K. Demerjian, *Atmos. Environ.* **10**, 459 (1976); J. Peterson, *ibid.* **11**, 689 (1977); R. Dickerson, D. Stedman, A. Delany, *J. Geophys. Res.* **87**, 4933 (1982); T. Blackburn, S. Bairai, D. Stedman, *ibid.* **97**, 10109 (1992); A. Ruggaber, R. Dlugi, T. Nakajima, *J. Atmos. Chem*. **18**, 171 (1994); C. Blindauer, V. Rozanov, J. Burrows, *ibid.* **24**, 1 (1996).
3. R. E. Shetter *et al*., *J. Geophys. Res*. **101**, 14631 (1996)
4. The impact of aerosols on the amount of solar radiation reaching Earth's surface is quantified by the aerosol optical depth (τ), defined as $\tau = \ln (I_o/I) \cos \theta$, where θ is the solar zenith angle, I is the observed direct solar radiance at Earth's surface, and I_o is the same radiance under an aerosol-free atmosphere. When τ equals or exceeds unity, the atmosphere is said to be optically thick [R. J. Charlson *et al*., *Science* **255**, 423 (1992); J. T. Kiehl and B. P. Briegleb, *ibid.* **260**, 311 (1993); J. T. Houghton *et al*., *Climate Change 1995: The Science of Climate Change* (Cambridge Univ. Press, Cambridge, 1996)].
5. C. Bruehl and P. J. Crutzen, *Geophys. Res. Lett.* **16**, 703 (1989).
6. S. Madronich, *J. Geophys. Res.* **92**, 9740 (1987).
7. The photolysis rate coefficients presented here were determined with an instrument described by P. Kelley, R. Dickerson, W. Luke, and G. Kok [*Geophys. Res. Lett.* **22** (no. 19), 2621 (1995)]. Most natural surfaces (except snow) reflect 8% or less of incident UV irradiance. For these measurements, a black surface was placed below the actinometer to ensure a constant and known local albedo, ensuring that radiation was measured only from the downwelling 2π steradians. This device has an absolute uncertainty of about 7% at the 95% confidence level for zenith angles less than 60°; the precision is a few percent.
8. K. L. Civerolo, thesis, University of Maryland, College Park, MD (1996); W. Ryan, B. Doddridge, R. Dickerson, K. Hallock, *J. Air Waste Manage. Assoc.*, in press.
9. The instruments monitor direct solar radiation and sky radiance at the almucanter (on the celestial circle parallel to the horizon and at the same zenith angle as the sun) and principal plane (the plane perpendicular to the horizon through the apparent position of the sun) [Y. Kaufman *et al*., *J. Geophys. Res*. **99**, 10341 (1994); T. Nakajima *et al*., *Appl. Opt.* **35**, 2672 (1996); B. N. Holben *et al*., Sixth International Symposium of Physical Measurements and Signatures in Remote Sensing, Val D'Isere, France, 17 to 21 January 1994 (Center National d'Etudes Spatiales, Toulouse, France, 1997), pp. 75–83; L. Remer, S. Gasso, D. Hegg, Y. Kaufman, B. Holben, *J. Geophys. Res.*, **102**, 16849 (1997).
10. E. Flowers, R. McCormick, K. Kurfis, *J. Appl. Meteorol.* **8**, 955 (1969); J. Peterson, E. Flowers, G. J. Berri, C. L. Reynolds, J. H. Rudisill, *ibid.* **20**, 229 (1981); R. B. Husar, J. M. Holloway, D. E. Patterson, W. E. Wilson, *Atmos. Environ*. **15**, 1919 (1981); Y. Kaufman and R. S. Fraser, *J. Appl. Meteorol.* **22**, 1694 (1983); R. B. Husar and W. E. Wilson, *Environ. Sci. Technol.* **27**, 12 (1993).
11. A large fraction of atmospheric particles are formed by photochemical reactions, but reduction of NO_x and NMHC emissions may not lead to proportionate reductions in particulate loading [J. R. Odum, T. P. W. Jungkamp, R. J. Griffin, R. C. Flagan, J. H. Seinfeld, *Science* **276**, 96 (1997); Z. Meng, D. Dabdub, J. H. Seinfeld, *ibid.* **277**, 116 (1997)].
12. R. Fraser and Y. Kaufman, *J. Geosci. Rem. Sens.* **23**, 525 (1985); Y. Kaufman, T. Brakke, E. Eloranta, *J. Atmos. Sci.* **43** (no. 11), 1135 (1986).
13. W. Wiscombe, *Appl. Opt.* **19**, 1505 (1980).
14. K. Stamnes, S.-C. Tsay, W. Wiscombe, K. Jayaweera, *Appl. Opt.* **27** (no. 12), 2502 (1988).
15. NASA Jet Propulsion Laboratory, Chemical Kinetics and Photochemical Data for use in Stratospheric Modeling, Evaluation No. 11, 1994.
16. S. Kondragunta, thesis, University of Maryland, College Park, MD (1997).
17. J. Lelieveld and P. J. Crutzen, *Nature* **343**, 277 (1990); F. Dentener and P. Crutzen, *J. Geophys. Res.* **98** (no. 4), 7149 (1993); C. Walcek, H.-H. Yuan, W. Stockwell, *Atmos. Environ.* **31** (no. 8), 1221 (1997); J. Liang and D. Jacob, *J. Geophys. Res.* **102** (no. 5), 5993 (1997); M. Andreae and P. Crutzen, *Science* **276**, 1052 (1997); A. R. Ravishankara, *ibid.*, p. 1058.
18. D. Hauglustaine, B. Ridley, S. Solomon, P. Hess, S. Madronich, *Geophys. Res. Lett.* **23**, 2609 (1996); D. Lary *et al.*, *J. Geophys. Res.* **102**, 3671 (1997).
19. M. Naja and S. Lal, *Geophys. Res. Lett.* **23**, 81 (1996); C. Varshney and M. Aggarwal, *Atmos. Environ.* **26**, 291 (1992); J. Herman *et al*., *J. Geophys. Res.* **102**, 16911 (1997); K. Rhoads *et al*., *ibid*., p. 18981.

20. We thank P. Crutzen, Y. Kaufman, I. Laszlo, and W. Ryan for helpful comments. Supported by Electric Power Research Institute through the NARSTO-Northeast Program, by the National Science Foundation–funded Center for Clouds, Chemistry, and Climate, and by NASA EOS Interdisciplinary Science Investigation.

30 May 1997; accepted 23 September 1997